Frontiers of Materials Science

Electronic Supplementary Material

Oil bath chelation-assisted fabrication of nitrogen-doped carbon-coated Ni_9S_8/Ni_3S_2 composites for lithium-ion batteries

Liangbao Liu[1], Mingjun Pang (✉)[2], Xianfeng Zhu[1], Changyou Li[1], Hao Wang[1], Anyuan Wang[1], Yi Gong[1], Shang Jiang[2], and Jin Chai (✉)[1]

1 China Academy of Aerospace Aerodynamics, Beijing 100074, China
2 Engineering Research Center of Coal-based Ecological Carbon Sequestration Technology of the Ministry of Education, Shanxi Datong University, Datong 037009, China

E-mails: pangmingjun3714@163.com (M.P.), 3368376569@qq.com (J.C.)

Material characterization

A suite of characterization techniques was employed to thoroughly examine the structural and morphological properties of samples. Initially, XRD was performed using a Rigaku D/Max-III setup equipped with a Cu Kα source operated at 30 kV and 30 mA. Surface chemical compositions of samples were examined via XPS using a Thermo ESCALAB 250 XI system. HRTEM was conducted using a JEOL JEM-2010 microscope, while TEM and FESEM were carried out using a Hitachi-4800 microscope.

Electrochemical testing

A meticulous mixture was methodically prepared through grinding samples (i.e., N-NiS-1, N-NiS-2, N-NiS-3, and N-NiS-4) along with acetylene black and PVDF in a pestle with a mass ratio of 7:2:1, employing NMP as the solvent. This mixture was then subjected to a continuous grinding process until achieving a homogenous slurry consistency. Thereafter, the slurry was applied in a uniform manner onto a pristine copper foil, utilizing a spatula for this purpose. The substrate, which had been coated with the slurry, was then placed in a vacuum oven. There, it underwent a drying process at 100 °C for 10 h. Once the substrate was dried, it was carefully cut into uniform pieces measuring 1 cm by 1 cm. These pieces were then designated as the working electrodes, with each electrode containing approximately 1–2 mg of the active material. The construction of button cells (type CR2025) was then undertaken in an argon-saturated glove box environment, with Whatman glass fiber separators and lithium wafer serving as the counter electrode. Cells were then filled with the electrolyte composed of 1 $mol \cdot L^{-1}$ LiPF6 dissolved in a balanced mixture of EC, DEC, and DMC. Subsequently electrochemical behaviors of such cells were assessed using a CHI660 electrochemical workstation from Chenhua Instruments along with a Land battery-test system. Testing parameters were derived from both the cyclic voltammetry (CV) and the galvanostatic charging–discharging (GCD) tests. These tests were executed within a voltage window ranging from 0 to 3.00 V with the Li/Li^+ reference. Electrical impedance spectroscopy (EIS) was performed at open circuit voltages, covering a frequency spectrum from 100 kHz down to 0.01 Hz.

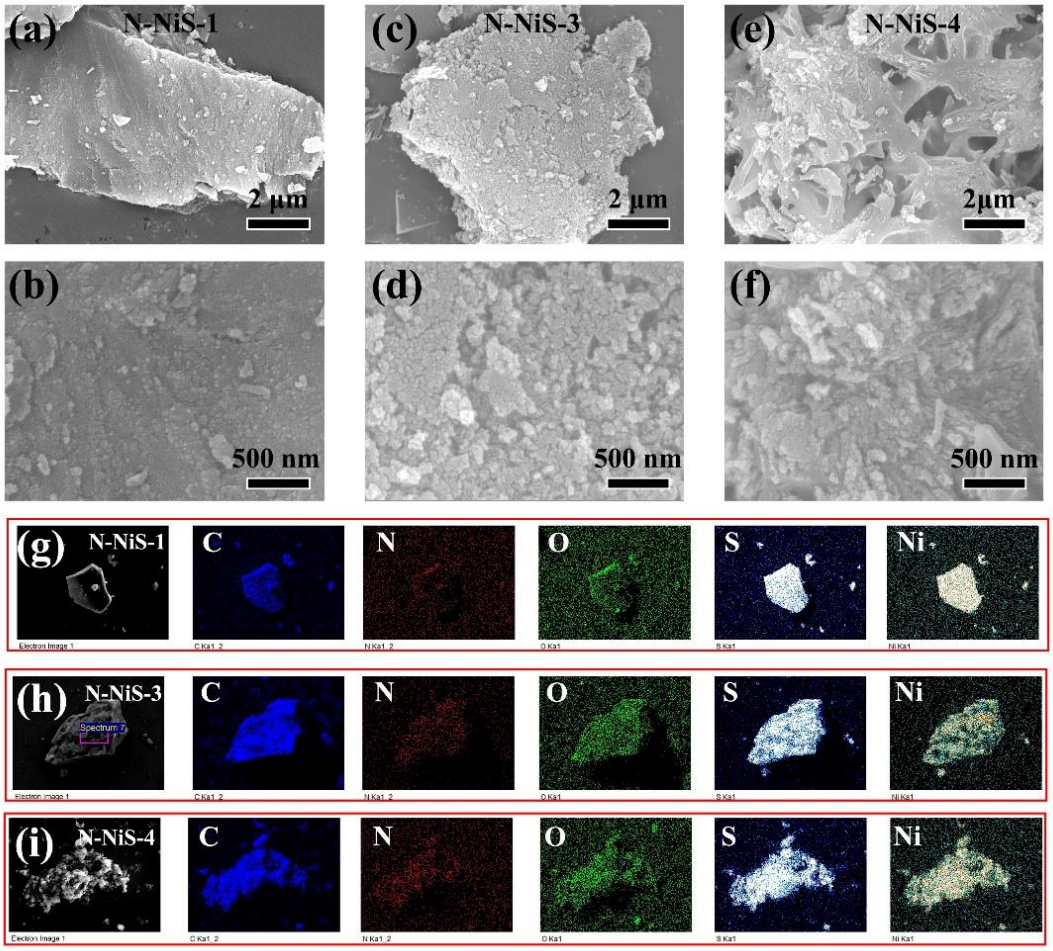

Fig. S1 (a)(b)(c)(d)(e)(f) SEM images of N-NiS-1 (left), N-NiS-3 (middle), and N-NiS-4 (right). **(g)(h)(i)** EDS elemental mapping images of N-NiS-1, N-NiS-3, and N-NiS-4.

Table S1 Fitting binding energy data of nickel and sulfur elements for N-NiS-2

Element	Binding energy/eV						
	Ni^{2+}	Ni^{3+}	Sat.	S_2^{2-}	C−S	C=S	SO_x^{n-}
Ni	853.19	856.11	861.33	–	–	–	–
	870.49	873.4	879.39	–	–	–	–
S	–	–	–	161.95	163.73	165.19	168.46

Table S2 Fitting binding energy data of carbon and nitrogen elements for N-NiS-2

Element	Binding energy/eV							
	C−C	C−S	C−O/N	O−C=O	Ni−N	Pyrrolic N	Graphitic N	N-oxide
C	284.39	284.99	285.85	288.33	–	–	–	–
N	–	–	–	–	398.43	399.81	400.84	403.67

Table S3 Comparison of rate performances for N-NiS-1, N-NiS-2, N-NiS-3, and N-NiS-4 under different current densities

Sample	Rate performance/(mAh·g^{-1})									
	50 [a)]	100 [a)]	200 [a)]	300 [a)]	500 [a)]	800 [a)]	1000 [a)]	1500 [a)]	2000 [a)]	50 [a)]
N-NiS-1	564.2	514.7	468.9	422.6	407.7	344.4	321.6	290.4	286.7	524.1
N-NiS-2	677.6	590.1	559	490.7	419.4	364.3	343.3	312.1	307.2	618.2
N-NiS-3	587.1	529.4	443.8	379.3	365.5	320	295	273.8	239.1	538
N-NiS-4	536.7	497.6	436.5	397.8	365.3	338.4	301.3	283.6	245.3	517.7

a) The unit of the current density is mA·g^{-1}.

Table S4 Comparison of electrochemical properties for derived sulfides between this work and previous reports

Sample	Ref.	Electrochemical performance	High-current cyclic performance
N-NiS-2	This work	677.6 mAh·g^{-1} at 0.05 A·g^{-1}	420.1 mAh·g^{-1} at 0.5 A·g^{-1} after 500 cycles [a)]
NiS/$Ni_3(BO_3)_2$/NC	[S1]	684 mAh·g^{-1} at 0.2 A·g^{-1}	322 mAh·g^{-1} at 1 A·g^{-1} after 500 cycles
Co@Ni_3S_2	[S2]	619.4 mAh·g^{-1} at 0.06 A·g^{-1}	531 mAh·g^{-1} at 0.06 A·g^{-1} after 50 cycles
Ni_3S_2-NCNFs	[S3]	658.1 mAh·g^{-1} at 0.1 A·g^{-1}	487.1 mAh·g^{-1} at 0.1 A·g^{-1} after 600 cycles
NiSe@N-doped C	[S4]	442 mAh·g^{-1} at 0.2 A·g^{-1}	262 mAh·g^{-1} at 2 A·g^{-1} after 300 cycles
Ni−Co−S-0.5/NC	[S5]	718.4 mAh·g^{-1} at 0.1 A·g^{-1}	755 mAh·g^{-1} at 0.2 A·g^{-1} after 200 cycles
Ni_3S_4 QDs	[S6]	602 mAh·g^{-1} at 0.1 A·g^{-1}	522.2 mAh·g^{-1} at 0.5 A·g^{-1} after 500 cycles
NiS@NSC	[S7]	601.2 mAh·g^{-1} at 0.1 A·g^{-1}	715.9 mAh·g^{-1} at 0.1 A·g^{-1} after 200 cycles
NiS/CPC	[S8]	650 mAh·g^{-1} at 0.1 A·g^{-1}	600 mAh·g^{-1} at 0.1 A·g^{-1} after 50 cycles

a) The retention ratio is 110.1%.

Table S5 Comparison of impedance fitting data before and after cycling for N-NiS-1, N-NiS-2, N-NiS-3, and N-NiS-4

Sample	Before cycling		After cycling		
	R_s/Ω	R_{ct}/Ω	R_s/Ω	R_{SEI}/Ω	R_{ct}/Ω
N-NiS-1	4.589	323.7	10.03 ↑	22.08	74.65 ↓
N-NiS-2	141.6	420.4	5.171 ↓	4.172	32.46 ↓
N-NiS-3	3.975	282	8.232 ↑	19.12	34.57 ↓
N-NiS-4	4.762	402.9	3.782 ↓	15.33	42.96 ↓

References

[S1] Yu Z, Abidin S Z, Toyong N M P, et al. Rational design of N-doped C-encapsulated flower-like nickel-based heterostructured microsphere anodes for high-capacity and stable lithium storage. Dalton Transactions, 2024, 53(4): 1497–1505

[S2] Chen X, Huang Y, Han X, et al. Synthesis of cobalt nanofibers@nickel sulfide nanosheets hierarchical core–shell composites for anode materials of lithium ion batteries. Electrochimica Acta, 2018, 284: 418–426

[S3] Guan M, Li Z, Ouyang J, et al. A facile electrospinning strategy for fibrous Ni_xS_y quantum dots@N doped carbon nanofibers as high-performance Li-ion battery anodes. Materials Today Communications, 2022, 31: 103652

[S4] Gao T P, Wong K W, Ng K M. Impacts of morphology and N-doped carbon encapsulation on electrochemical properties of NiSe for lithium storage. Energy Storage Materials, 2020, 25: 210–216

[S5] Yi M, Zhang C, Cao C, et al. MOF-derived hybrid hollow submicrospheres of nitrogen-doped carbon-encapsulated bimetallic Ni–Co–S nanoparticles for supercapacitors and lithium ion batteries. Inorganic Chemistry, 2019, 58(6): 3916–3924

[S6] Chen W, Zhang X, Peng Y, et al. One-pot scalable synthesis of pure phase Ni_3S_4 quantum dots as a versatile electrode for high performance hybrid supercapacitors and lithium ion batteries. Journal of Power Sources, 2019, 438: 227004

[S7] Dong X, Deng Z P, Huo L H, et al. Large-scale synthesis of NiS@N and S co-doped carbon mesoporous tubule as high performance anode for lithium-ion battery. Journal of Alloys and Compounds, 2019, 788: 984–992

[S8] Vadivazhagan M, N. K. S, Nallathamby K. Demonstration of biocarbon-added NiS porous nanospheres as a potential anode for lithium-ion batteries. Energy & Fuels, 2021, 35(10): 8991–9000